Acta Crystallographica Section D
Biological Crystallography
ISSN 0907-4449

Structure of β-cinnamomin, a protein toxic to some plant species

Maria L. Rodrigues,[a] Margarida Archer,[a] Paulo Martel,[a,b] Alain Jacquet,[c] Alfredo Cravador[b] and Maria A. Carrondo[a]*

[a]Instituto de Tecnologia Química e Biológica, Universidade Nova de Lisboa, ITQB-UNL, Av. República, Apt 127, 2781-901 Oeiras, Portugal, [b]Universidade do Algarve, FERN, Campus de Gambelas, 8000-117 Faro, Portugal, and [c]Universite Libre de Bruxelles, Service de Génétique Appliquée, IBMM, ULB, Rue des Professeurs Jeener et Brachet 12, B-6041 Gosselies, Belgium

Correspondence e-mail: carrondo@itqb.unl.pt

Received 6 February 2002
Accepted 6 June 2002

PDB Reference:
β-cinnamomin, 1ljp, r1ljpsf.

Phytophthora and *Pythium* species are among the most aggressive plant pathogens, as they invade many economically important crops and forest trees. They secrete large amounts of 10 kDa proteins called elicitins that can act as elicitors of plant defence mechanisms. These proteins may also induce a hypersensitive response (HR) including plant cell necrosis, with different levels of toxicity depending on their pI. Recent studies showed that elicitins function as sterol carrier proteins. The crystallographic structure of the highly necrotic recombinant β-cinnamomin (β-CIN) from *Phytophthora cinnamomi* has been determined at 1.8 Å resolution using the molecular-replacement method. β-CIN has the same overall structure as β-cryptogein (β-CRY), an elicitin secreted by *Phytophthora cryptogea*, although it shows a different surface electrostatic potential distribution. The protein was expressed in *Pichia pastoris* and crystallized in the triclinic space group with two monomers in the asymmetric unit. The interface formed by these two monomers resembles that from β-CRY dimer, although with fewer interactions.

1. Introduction

Plant diseases caused by the oomycetous fungi, actually phylogenetically classified with the heterokont algae (Kumar & Rzhetsky, 1996), of *Phytophthora* (*P.*) species involve thousands of plant species and are spread worldwide. The genus comprises approximately 60 species, almost all destructive pathogens that cause rot in roots, stems, leaves and fruits of a large range of agricultural and ornamentally important plant hosts. Examples of outbreaks leading to crop and forest devastation of catastrophic economical and social consequences abound (Bourke, 1991; Large, 1940; Gregory, 1983; Podger *et al.*, 1965; Podger, 1972; Shea *et al.*, 1983; McBlain, Hacker *et al.*, 1991; McBlain, Zimmerly *et al.*, 1991; Evans & Prior, 1987). Recently, the decline of *Quercus suber* (*Q. suber*) and *Q. ilex* in Portugal and Spain has been associated with infection by *P. cinnamomi* (Brasier, 1992; Brasier *et al.*, 1993; Sánchez *et al.*, 2002) causing widespread deaths of cork oak and cork holm, and threatening oak ecosystems. Most *Phytophthora* species studied secrete large amounts of elicitins, a group of unique highly conserved proteins. Elicitin-like proteins have also been detected in some *Pythium* (*Py.*) species such as *Py. vexan* or *Py. oligandrum* (Huet *et al.*, 1995; Panabières *et al.*, 1997).

Since the isolation and primary structure determination of the first elements of this novel class of proteins (Huet & Pernollet, 1989; Ricci *et al.*, 1989), a great research effort has been directed towards the study of their chemistry and physiological effects (for reviews, see Grant *et al.*, 1996; Ponchet *et al.*, 1999). These polypeptides are holoproteins of

98 residues ($M_r \simeq 10\,300$) whose amino-acid composition shows some particular features, namely six Cys residues participating in three S—S bridges at conserved positions, an absence of Arg, His and Trp, and a high content of Ser and Thr. They are classified as acidic, α, or basic, β, proteins according to their pI (α, pI < 5.0; β, pI > 7.5), mainly determined by the number of Lys residues. The physiology of elicitin activity was extensively studied in tobacco plants, where they were shown to induce a systemic acquired resistance (SAR) against fungal and bacterial pathogens, accompanied by limited leaf necrosis (Ricci *et al.*, 1989; Yu, 1995). Moreover, elicitins can stimulate natural defences in some other plant species, such as tomato, which upon inoculation with oligandrin (from *Py. oligandrum*) becomes resistant to *P. parasitica* (Picard *et al.*, 2000). Transgenic tobacco plants that produce cryptogein upon challenge with virulent *P. parasitica* var. *nicotianae* were shown to develop an HR and to be resistant to disease caused by fungal pathogens unrelated to *Phytophthora* species (Keller *et al.*, 1999)

The necrotic activity of α- and β-elicitin isoforms has been studied on leaves of tobacco plants and suggested that the degree of necroticity is related to the nature of the amino acid at position 13: a hydrophilic residue in β-elicitins, usually a lysine, and a hydrophobic residue in α-elicitins, a valine (Ricci *et al.*, 1989; Huet *et al.*, 1992, 1994; Nespoulous *et al.*, 1992; Kamoun *et al.*, 1993; Pernollet *et al.*, 1993). These studies show that β-elicitins are more necrotic than α-elicitins, β-CIN being the most necrotic (Pernollet *et al.*, 1993).

Further potential elicitor and/or necrotic sites were identified, namely at positions 2, 22, 25, 28, 39, 61, 70, 72, 93, 94 and 96, either by sequence comparisons, site-directed mutagenesis (Perez *et al.*, 1999; Duclos, Trincão Aurélio *et al.*, 1998) or using synthetic peptides and tobacco plants transformed with a reporter gene (GUS) controlled by defence-gene promoters (Perez *et al.*, 1997). Nevertheless, the role of elicitins in plant–pathogen interactions is not yet fully understood and further studies are required to develop resistance in plants.

The three-dimensional crystal structure of wild-type cryptogein was determined, revealing a polypeptide chain with a novel folding type (Boissy *et al.*, 1996). Subsequently, the three-dimensional structure of a recombinant K13H-mutated cryptogein revealed a molecule of ergosterol enclosed in a hydrophobic cavity of the polypeptide (Boissy *et al.*, 1999). This finding is in accordance with previous studies suggesting that elicitins are a new class of sterol carrier proteins (Mikes *et al.*, 1997, 1998) and are able to sequester sterols from plant plasma membranes and transfer them to and from lipid micelles (Vauthrin *et al.*, 1999). Elicitins can also bind fatty acids, although with significantly lower affinity (Osman, Mikes *et al.*, 2001). In an attempt to elucidate the recognition of these elicitor proteins by the plant host, putative high-affinity binding sites were identified in tobacco plasma membranes (Wendehenne *et al.*, 1995) and later characterized as glycoproteins (Bourque *et al.*, 1999).

Recent studies have further suggested that the sterol carrier capacity and elicitor activity are correlated (Ponchet *et al.*, 1999) and the formation of a sterol–elicitin complex is a prerequisite step before elicitins bind to their putative receptors and induce cell-defence responses (Osman, Vauthrin *et al.*, 2001).

Table 1
Crystallographic data and refinement statistics.

Values in parentheses are for the highest resolution shell (1.86–1.80 Å).

Crystallographic data	
Space group	*P*1
Unit-cell parameters (Å, °)	$a = 31.85$, $b = 36.91$, $c = 43.93$, $\alpha = 77.64$, $\beta = 86.67$, $\gamma = 79.55$
Resolution range (Å)	21.4–1.8
Total No. of reflections	61726
No. of unique reflections	16756
Redundancy	3.7
Reflections with $I/\sigma(I) > 3$ (%)	93.7 (77.4)
Completeness (%)	94.3 (90.3)
$R_{\rm merge}$ (%)	3.6 (12.1)
Refinement statistics	
$R_{\rm factor}$ (%)	19.8
$R_{\rm free}$ (%)	21.9
Total No. of protein non-H atoms	1428
No. of water molecules	201
Average *B* factor (Å^2)	
All protein atoms	18.8
Main-chain atoms	17.6
Side-chain atoms	20.2
Solvent	28.8
R.m.s.d. from ideal value	
Bond lengths (Å)	0.004
Bond angles (°)	1.043
Dihedral angles (°)	19.092
Improper angles (°)	0.652

As part of a programme to investigate *P. cinnamomi*–*Q. suber* interactions at the molecular level, namely to investigate the role of β-cinnamomin in the pathogenesis process and to contribute to the elucidation of the biological functions of these holoproteins, we have recently identified an elicitin gene cluster in *P. cinnamomi* (Duclos, Fauconnier *et al.*, 1998), constructed a synthetic gene on the basis of the amino-acid sequence of β-cinnamomin, expressed it (Duclos, Trincão Aurélio *et al.*, 1998) and crystallized the recombinant protein (Archer *et al.*, 2000).

We report here the crystal structure of β-cinnamomin (β-CIN). The three-dimensional structure of β-CIN is similar to the structure of β-cryptogein (β-CRY). Owing to the high amino-acid sequence homology among elicitins, it is expected that the overall fold should be conserved within this family of proteins. More structural information is important to contribute to a better understanding of the interactions between plants and this type of pathogen.

2. Experimental

2.1. Purification, crystallization and data collection

β-CIN was expressed in the methylotrophic yeast *Pichia pastoris* as described in Archer *et al.* (2000). The purified recombinant protein was crystallized using either polyethyleneglycol (PEG) or ammonium sulfate as precipitants at a pH around 7. Both conditions gave isomorphous crystals

that belong to the triclinic space group (Archer *et al.*, 2000). X-ray diffraction of a frozen crystal was measured at 1.8 Å resolution using a copper rotating-anode generator.

The crystal has unit-cell parameters a = 31.85, b = 36.91, c = 43.93 Å, α = 77.64, β = 86.67, γ = 79.55°. The reflections were integrated and scaled with the program suite *HKL* (Otwinowski & Minor, 1997). The asymmetric unit contains two molecules of β-CIN, corresponding to a solvent content of about 49%. Relevant processing statistics are presented in Table 1.

2.2. Structure solution and model refinement

The structure of β-CIN was determined by molecular replacement with the program *AMoRe* (Navaza, 1994), using the coordinates of β-cryptogein (PDB code 1beo) as a search model. Calculations were performed over the resolution range 15–3.5 Å. Rigid-body refinement within *AMoRe* gave a correlation coefficient of 49.4% and an R factor of 41.0% for the correct solution (values for the second ranked solution were 15.8% for the correlation coefficient and 52.8% for the R factor).

Structure refinement was carried out with *CNS* (Brünger *et al.*, 1998) using the maximum-likelihood 'mlf' target function. For cross-validation, 5% of randomly selected reflections were kept apart. The graphic program *TURBO* (Roussel & Cambillau, 1989) was used for map inspections and manual model building.

Initial steps of refinement included the WarpNTrace option of the *ARP/wARP* program (Perrakis *et al.*, 1999) to optimize the position of a region on the Ω-loop (residues 33–39) and simulated annealing with *CNS* using strict non-crystallographic symmetry (NCS) constraints. Energy minimization proceeded first with restrained NCS of successively decreasing restraint strength and finally with total release of the restraints, monitored by evolution of R and $R_{\rm free}$ values. All refinement calculations were performed using diffraction data to 1.8 Å. No cutoff on the low-resolution data was applied in the bulk-solvent correction. After individual B-factor refinement, water molecules were introduced with the WATERPICK routine of *CNS*.

The final model includes all the 98 residues for both monomers and 201 water molecules, corresponding to a total of 1629 non-H atoms. The R factor and $R_{\rm free}$ values converged to 19.8 and 21.9%, respectively. Refinement statistics are summarized in Table 1.

3. Results and discussion

3.1. Analysis of elicitin sequences

A scan of the PIR-NREF database (Barker *et al.*, 2001) against the β-cinnamomin sequence matched 32 sequences with significant homology scores, 26 of which are unique. The sequences were aligned with the multiple alignment program *CLUSTALX* (Thompson *et al.*, 1994) and a cluster analysis based on the identity matrix was performed with the *MODELLER* program (Sali & Blundell, 1993). Almost all primary sequences show pairwise identities above 65% and the sequence alignment reveals several highly conserved regions (residues 7–9, 15–20, 31–38, 40–43, 50–51, 53–56, 69–85 and 95–98; Fig. 1). This high level of identity suggests a very similar three-dimensional structure and makes the elicitins excellent candidates for homology modelling (Marti-Renom *et al.*, 2000).

Three sequences stand out from the set, oligandrin (from *Py. oligandrum*) and infestins 2A and 2B (from *P. infestans*) and therefore are not included in the alignment. Infestins display identities in the range 50–60% when compared with the remaining sequences (however, the alignment corresponds

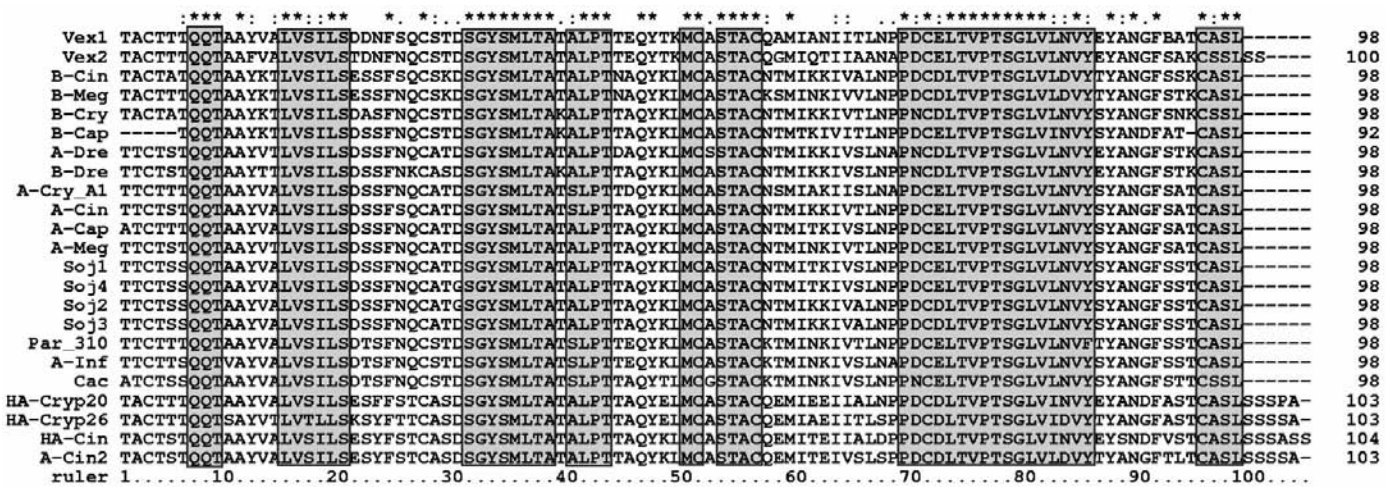

Figure 1
Amino-acid sequences alignment of the 23 elicitins, from *Pythium* (*Py.*) and *Phytophthora* (*P.*) species that share pairwise identities above 65%. *, identity; :, strongly similar; ., weakly similar. The elicitin sequences were determined from the following organisms: Vex1 and Vex2, *Py. vexans*; B-Cin, A-Cin, HA-Cin and A-Cin2, *P. cinnamomi*; B-Meg and A-Meg, *P. megasperma*; B-Cry, A-Cry_A1, HA-Cryp20 and HA-Cryp26, *P. cryptogea*; B-Cap (fragment) and A-Cap, *P. capsici*; A-Dre and B-Dre, *P. drescheleri*; Soj1, Soj2, Soj3 and Soj4, *P. sojae*; Par_310, *P. parasitica*; A-Inf, *P. infestans*; Cac, *P. cactorum* (A, acidic elicitin; B, basic elicitin; HA, highly acidic). Sequence lengths are indicated in the far right column.

to a small fraction of the total length of these 195 and 198 amino-acid sequences), while oligandrin is a more distant relative (identities between 36 and 43%).

3.2. Structure analysis

The final model of β-CIN comprises all 98 residues for each monomer (*A* and *B*) in the asymmetric unit. The electron density is well defined for most of the protein, with some exceptions: Thr1 in both monomers, Ser34 and Met35 of molecule *B* and a few surface polar residues.

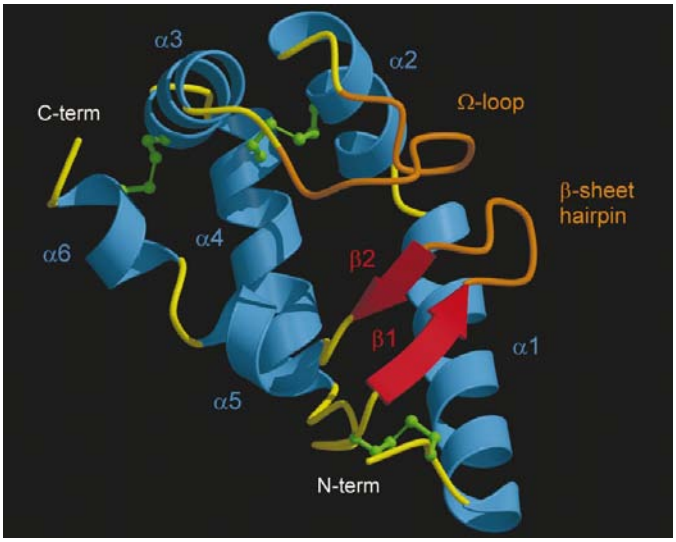

Figure 2
Secondary-structure representation of β-CIN monomer. Helices are represented in blue, β-sheet is coloured red and cysteine side chains forming the disulfide bridges are green. The beak-like motif, which is composed of the Ω-loop and the β-sheet hairpin loop regions, is coloured orange. Figure generated using the programs *MOLSCRIPT* (Kraulis, 1991) and *Raster3D* (Merritt & Bacon, 1997).

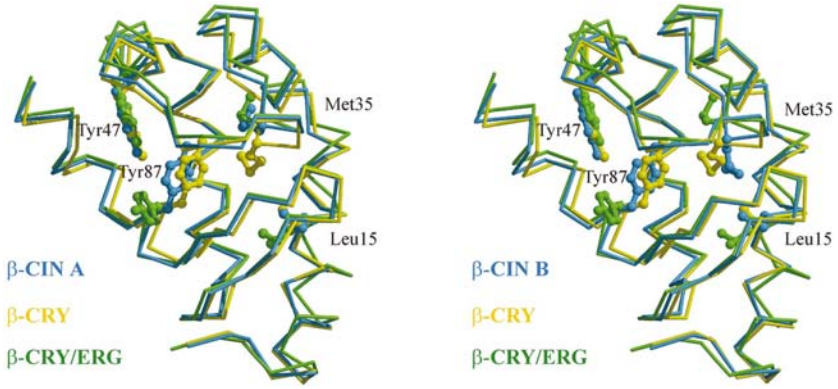

Figure 3
C^{α}-atoms superposition for each monomer of β-CIN (β-CIN *A* and β-CIN *B*) with the two crystallographic structures of β-CRY, the ligand-free protein (β-CRY; PDB code 1beo) and the mutated protein complex with ergosterol (β-CRY/ERG; PDB code 1bxm). Several residues are represented in ball-and-stick, namely Tyr47 and those that undergo major changes upon sterol binding: Leu15, Met35 and Tyr87. The ergosterol molecule is not shown for the sake of clarity. Figure drawn with the programs *MOLSCRIPT* (Kraulis, 1991) and *Raster3D* (Merritt & Bacon, 1997).

In general, the two monomers are very similar (r.m.s. deviations of 0.32 Å for main-chain and 0.63 Å for all protein atoms), differing essentially through residues 34–39 (with a largest main-chain r.m.s.d. of 1.4 Å for Ser34 and a side-chain r.m.s.d. of 4.4 Å for Met35). Not surprisingly, this region is expected to have a higher flexibility since it belongs to the loop that forms a lid over the ligand cavity of elicitins (Boissy *et al.*, 1999). This mobility is also observed in the NMR solution structure of cryptogein (Fefeu *et al.*, 1997).

Inspection of the Ramachandran plot (Ramachandran & Sasisekharan, 1968) as defined by the program *PROCHECK* (Laskowski *et al.*, 1993) shows six residues (Asn67*A*/*B*, Asp70*A*/*B*, Ser34*A* and Ser78*A*) in the additionally allowed regions, corresponding to 3% of the total structure.

3.3. Overall structure

The overall structure of β-CIN is rather similar to that of β-CRY (Boissy *et al.*, 1996) and is probably representative of the elicitin family. A ribbon representation of the secondary structure of β-CIN is shown in Fig. 2. It comprises six α-helices, a short two-stranded β-sheet and a large Ω-loop (Tyr33–Pro42). Three disulfide bonds (Cys3–Cys71, Cys27–Cys56 and Cys51–Cys95) strengthen this fold. Two ionic interactions, N-terminus–Asp72 and Asp21–Lys62, are thought to be important in the stabilization of the β-CRY structure (Gooley *et al.*, 1998). In β-CIN, the first interaction is conserved, while the second is mediated by a water molecule between Glu21 and Lys62, although the main-chain atom positions of both residues remain almost the same in the two structures.

The so-called 'beak-like motif' formed by the Ω-loop, the β-sheet and its associated hairpin loop borders a large internal hydrophobic cavity. In the structure of the mutant K13H of β-CRY this cavity accommodates ergosterol, a small ligand molecule (Boissy *et al.*, 1999). All residues in the beak-like motif region (residues 33–42 and 72–82) are strictly conserved among elicitins, except for residue 39, which in most elicitins, including β-CIN, is a threonine instead of a lysine (Fig. 1).

As previously noted (Boissy *et al.*, 1996), elicitins are structurally unrelated to any known protein family, thus displaying a new fold. Submission of the β-CIN coordinates to the DALI fold comparison software (Holm & Sander, 1993) matched β-CRY with a *Z* score of 19.2. The second hit, cole1 primer repressor, whose structure consists of two α-helices, matched β-CIN with a low *Z* score (3.4) and has no biological or functional analogy with elicitins.

3.4. Comparison with other elicitin structures

β-CIN is the second elicitin to be structurally characterized. With the objective of analyzing the structural details that may account for the small differences in biological activity between

β-CIN and β-CRY and that result from ligand binding, we shall compare the structures of the two native proteins with that of the mutated K13H β-CRY bound with ergosterol (Boissy *et al.*, 1999). The superposition of the 98 C^{α} atoms of chains *A* and *B* of β-CIN with β-CRY and β-CRY–ergosterol is shown in Fig. 3. As illustrated in the figure, the three molecules are very similar. The overall structural differences are somewhat higher between β-CIN and the complex (r.m.s.d. for C^{α} atoms of 0.89 Å for molecule *A* and 0.92 Å for molecule *B*) than between β-CIN and β-CRY (r.m.s.d. for C^{α} atoms of 0.62 Å for molecule *A* and 0.54 Å for molecule *B*). The higher discrepancy between β-CIN and β-CRY–ergosterol complex mainly arises from the deformation of helix α1 in the complex structure. Bending of helix α1 is one of the major conformational changes that occur upon ligand binding (Boissy *et al.*, 1999).

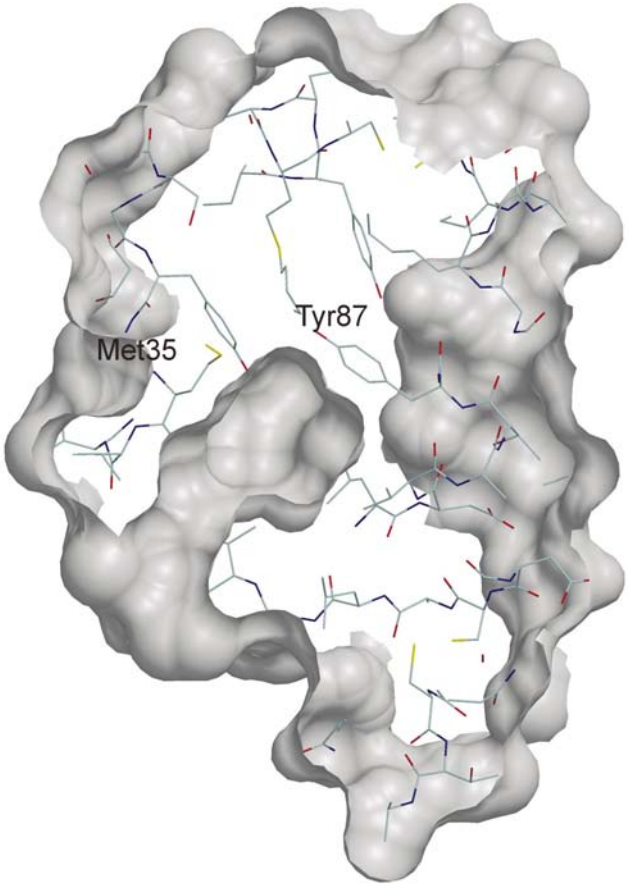

Figure 4
Section through the β-CIN molecule (monomer *A*) showing the internal hydrophobic cavity and its probable entrance (between helix α1 and the beak-like motif). Residue Tyr87 is clearly at the bottom of the internal surface, limiting the cavity. Conformation adopted by Met35 corresponds to the opening of this cavity. This orientation corresponds to a rotation of about 180° relative to the molecules represented in Fig. 3.

On one hand, the Ω-loop region of monomer *A* shows a lower structural similarity with the native cryptogein (average difference of 1.3 Å for the C^{α} atoms for residues 33–39, with a maximum value of 2.5 Å for Ser34) than with the β-CRY–ergosterol complex (average difference of 0.5 Å for the same Cα atoms) (Fig. 3). On the other hand, the Ω-loop region of monomer *B* is slightly closer to the native cryptogein than to the complex structure (average differences of 0.7 Å and of 0.9 Å, respectively).

The comparison of both CRY structures (free and bound) shows that Leu15, Met35 and Tyr87 are the residues that undergo major conformational changes upon ligand binding. It is worthwhile to note that in β-CIN the conformation adopted by Met35 in monomer *A* is equivalent to that observed in the complex structure (Fig. 3), facilitating an eventual access to the internal cavity, whereas in monomer *B* this residue is in a similar position to that of the native β-CRY structure. Fig. 4 represents a section through the β-CIN *A* molecule, showing the size and shape of this internal cavity. The alternative conformation of the Met35 side chain, as observed in molecule *B* and in the native β-CRY structure, limits the entrance to that cavity and significantly reduces its size. In both β-CIN molecules the side chains of Leu15 and Tyr87 have similar conformations to those of the native cryptogein structure, limiting access and binding of a ligand (Fig. 3). Therefore, bending of helix α1 and alterations in the side-chain conformations of Leu15 and Tyr87 may be solely correlated with ligand binding, while conformational changes in some residues of the Ω-loop, in particular Met35, may be related to the flexibility of this region, although a conformational change is certainly needed to allow the ligand entry into the hydrophobic cavity.

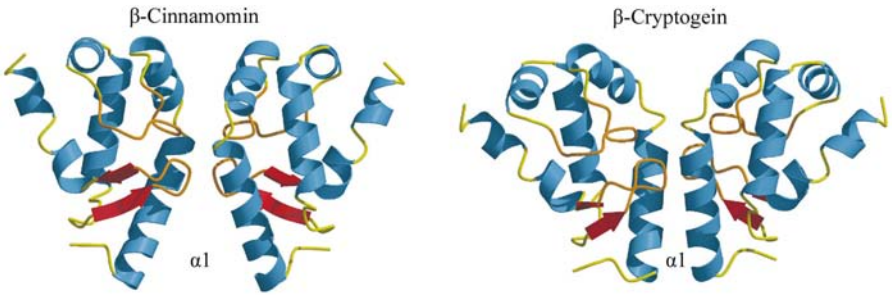

Figure 5
Comparative representation of the dimeric X-ray structures of β-CIN and β-CRY (PDB code 1beo). The helices α1 of each monomer of β-CIN are further apart compared with those of β-CRY. Figure drawn with *MOLSCRIPT* (Kraulis, 1991) and *Raster3D* (Merritt & Bacon, 1997).

Another residue involved in ligand binding is Tyr47, since it establishes a hydrogen bond with the hydroxyl group of ergosterol as shown in the β-CRY complex structure (Boissy *et al.*, 1999). In order to assess the relationship between sterol loading and elicitor properties, mutagenesis studies and binding experiments were performed on Tyr47 and Tyr87 in β-CRY (Y47F/G and Y87F), since they were thought to be important in sterol binding (Osman, Vauthrin *et al.*, 2001). The mutation Y47F was found to slightly affect the dissociation constant (K_d) of elicitin–sterol complexes, whereas

the Y47G mutation strongly increases this constant, meaning that the hydrogen bond and especially the van der Waals interactions are important for ligand stabilization. This residue is in a very similar conformation in the three crystal structures represented in Fig. 3 and is therefore ready to accept, in the native proteins, a sterol molecule in the interior cavity. An even more drastic increase in K_d is observed with the Y87F mutation (Osman, Vauthrin *et al.*, 2001). Phenylalanines are normally located in hydrophobic interior regions of protein structures, avoiding any contact with the solvent. Therefore, it is presumable that this aromatic side chain on the Y87F mutant may keep the same orientation as those of the equivalent residues in the two native elicitin structures β-CIN and β-CRY, thus preventing adaptation of a ligand into the internal cavity of the mutated protein.

3.5. Homodimer interactions

The two molecules present in the asymmetric unit of β-CIN are related by a pseudo-twofold axis and thus form a crystallographic dimer. However, this homodimer is different from that observed in the crystal (Boissy *et al.*, 1996) and solution (Gooley *et al.*, 1998) structures of β-CRY. Fig. 5 compares the crystal dimers of both elicitins.

In β-CIN the dimer interface is based on a central core of hydrophobic interactions between residues located on helix α1 and on the beak-like motif, and one hydrogen bond between residues Thr77*A* and Ser20*B*. In the case of β-CRY, the dimer has more hydrophobic interactions in the interface core and is further flanked by hydrophilic interactions through the beginning of helix α1. Table 2 lists residues and distances (below a cutoff value of 5.0 Å) involved in dimer interactions in both elicitin structures. The central hydrophobic set of contacts is similar in both dimers, with two conserved pairs, Val16–Pro76 and Leu19–Leu19. Since the residues that constitute this hydrophobic core are highly conserved (Leu15, Val16, Leu19, Leu36, Pro76) (see Fig. 1) one may suggest an eventual relevance of dimerization to the elicitin biological activity. On the other hand, upon ligand binding most of these residues are involved in contacts with the ligand molecule. Therefore, this may be an alternative explanation for the conserved region from residue 15 to residue 20 observed within the elicitin family.

It was previously shown that the elicitin β-CRY is predominantly a dimer in concentrated aqueous solutions (in the millimolar range; Gooley *et al.*, 1998). The solution structure of this dimer (Gooley *et al.*, 1998) is essentially the same as that observed in the crystalline structure, where a crystallographic twofold axis correlates the two molecules. In order to assess the role of the elicitin dimerization on their necrotic activity, further investigation is needed since it is known that elicitins are monomeric at physiological nanomolar concentrations.

The comparison between the crystallographic homodimers of β-CIN and β-CRY shows some differences (Fig. 5). Analysis of the hydrophobic contacts in the β-CIN and β-CRY dimers indicates a stronger stabilization for the β-CRY dimer in terms of excluded surface area, interface gap volume and atomic solvation energy (calculated with the program *ASC*; Eisenhaber *et al.*, 1995). These results, together with the aforementioned similarity between solution and crystalline β-CRY dimers, suggest that the distinct conformation of the β-CIN dimer may just be an artifact of crystal packing rather than having any biological relevance. In both monomers, residue Lys13 located in helix α1 forms a salt bridge with the C-terminus of a symmetry-related molecule, modifying the position of the helix so as to prevent an extensive interaction between them as in the case of the β-CRY dimer.

However, it is worthwhile to point out that upon dimerization the access to the ligand-binding pocket located between helix α1 and the beak-like motif is blocked. Since the recognition

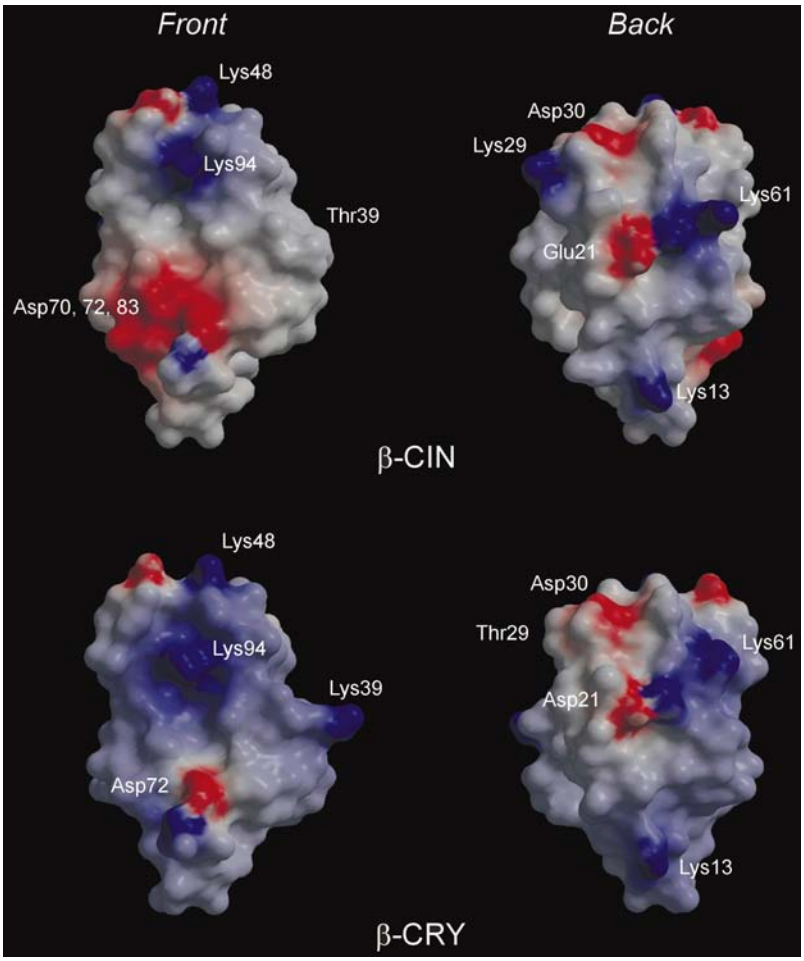

Figure 6
Surface electrostatic potentials of β-CIN and β-CRY (PDB code 1beo), front and back views. Negatively charged regions are represented in red and positively charged regions in blue. Figure created with the programs *GRASP* (Nicholls *et al.*, 1993) and *Raster3D* (Merritt & Bacon, 1997)

Table 2
Residues involved in dimer interactions in β-CIN and β-CRY X-ray structures.

β-CIN†			β-CRY‡		
Monomer *A*	Monomer *B*	Distance (Å)	Monomer *A*	Monomer *B*	Distance (Å)
			Ala5 O	Thr9 OG1	3.2
			Gln8 OE1	Lys13 NZ	3.7
Tyr12 CE1	Tyr12 CE1	3.7	Tyr12 CZ	Lys13 CG	3.4
			Tyr12 CD1	Val16 CG2	4.4
			Lys13 CG	Pro76 CG	3.7
			Leu15 CB	Val16 CG2	4.1
			Val16 CG2	Val16 CG2	3.8
			Val16 CG1	Leu19 CD1	4.3
			Val16 CG1	Leu36 CD1	4.5
Val16 CG1	Pro76 CB	3.9 (3.8)	Val16 CG1	Pro76 CG	3.9
Val16 CG1	Thr77 CG2	4.1 (3.9)	Val16 CG1	Thr77 CG2	4.8
Leu19 CD1	Leu19 CD1	4.4	Leu19 CD1	Leu19 CD1	3.5
Leu19 CD2	Leu36 CD1	4.1 (4.2)	Ser20 CG	Leu36 CD2	3.7
Leu19 CB	Thr77 CG2	3.8 (3.7)	Ser20 CG	Thr77 CG2	3.8
Phe24 CZ	Leu36 CG	4.1 (3.9)			
Leu36 CD1	Leu36 CD1	4.6			
Thr77 O	Ser20 OG	3.2			

† The equivalent interactions between the reverse residues from monomer *B* to monomer *A* have the distances quoted in parentheses. ‡ Equivalent interactions are observed between the reverse residues from monomer *B* to monomer *A* owing to the twofold crystallographic axis.

and eventually the penetration of a sterol molecule into that cavity occurs through this face of the protein molecule, one can speculate that the dimerization and ligand binding may be correlated. Dimerization may also be associated in some as yet unknown way with the possible existence of two elicitin localizations or domains, as extracellular and cell-wall-associated proteins (Ponchet *et al.*, 1999).

3.6. Surface electrostatic potential calculations

The calculated molecular electrostatic potentials at the surfaces of β-CIN and β-CRY calculated with the *GRASP* software (Nicholls *et al.*, 1993) are depicted in Fig. 6. The presence of two additional aspartate residues (at positions 70 and 83) in β-CIN compared with one (Asp72) in β-CRY creates a larger patch of negative charges, visible in the front representations, thus making the electrostatic potential at this side of both molecules very different. Two separate regions of negative and positively charged residues are seen in the front view of β-CIN, whereas in β-CRY this surface is mostly positive except for the negative patch of Asp72. These two regions include some of the 11 residues shown to be important for biological activity (Perez *et al.*, 1997): Ala2, Asp70 and Asp72 are located on the negative region, while Ser93, Lys94 and Ala96 correspond to the positive region. On the opposite side of the molecule, the potentials of β-CIN and β-CRY are much more similar, although the bottom region where Lys13 is located is more positive in β-CRY than in β-CIN. This side of the molecule also contains other putative active residues besides Lys13, namely three solvent-exposed serine residues (22, 25 and 28), and thus may be involved in a molecular interaction (Perez *et al.*, 1999).

It has been shown that in their respective classes, β-cinnamomin and α-cinnamomin are the most toxic elicitins against tobacco leaves (Pernollet *et al.*, 1993). Amino-acid sequence comparison and site-directed mutagenesis studies pointed out the important role of Ser25 in the high necrogenicity of both cinnamomins (Perez *et al.*, 1999). From analysis of the electrostatic potential, it is difficult to interpret this fact, since replacement of Ser25 by Asn (as in β-CRY) should not significantly change the molecular surface potential. On the other hand, the number of basic residues seems to correlate with the necrotic power of elictins, as evidenced by basic elictins being much more necrotic than the acidic elicitins. However, since β-CIN is less basic than β-CRY, its higher necrogenicity might be a consequence of a higher charge-distribution asymmetry at the molecular surface.

The authors are grateful to Dr Paul Gooley from the NMR Spectroscopy group of University of Melbourne for providing the coordinates of β-cryptogein solution dimer, and to Dr Pedro Matias for helpful discussions on technical aspects. This work was supported by project SAPIENS/34701/99 and grants PRAXIS XXI/BPD/17265/98 (MA), PRAXIS XXI/BIC/17185/98 and SFRH/BD/5228/2001 (MLR) from Fundação para a Ciência e a Tecnologia (FCT). We also thank FCT (PRAXIS XXI 3/3.2/FLOR/2112/95) and NATO (SfS PO-CORKOAKS II) for financial support.

References

Archer, M., Rodrigues, M. L., Aurelio, M., Biemans, R., Cravador, A. & Carrondo, M. A. (2000). *Acta Cryst.* D**56**, 363–365.
Barker, W. C., Garavelli, J. S., Hou, Z., Huang, H., Ledley, R. S., McGarvey, P. B., Mewes, H. W., Orcutt, B. C., Pfeiffer, F., Tsugita, A., Vinayaka, C. R., Xiao, C., Yeh, L. S. & Wu, C. (2001). *Nucleic Acids Res.* **29**, 29–32.
Boissy, G., de La Fortelle, E., Kahn, R., Huet, J. C., Bricogne, G., Pernollet, J. C. & Brunie, S. (1996). *Structure*, **4**, 1429–1439.
Boissy, G., O'Donohue, M., Gaudemer, O., Perez, V., Pernollet, J. C. & Brunie, S. (1999). *Protein Sci.* **8**, 1191–1199.
Bourke, A. (1991). In *Phytophthora*, edited by J. A. Lucas, R. C. Shuttock, D. S. Shaw & L. R. Cooke. Cambridge University Press.
Bourque, S., Binet, M. N., Ponchet, M., Pugin, A. & Lebrun-Garcia, A. (1999). *J. Biol. Chem.* **274**, 34699–34705.
Brasier, C. M. (1992). *Nature (London)*, **360**, 539.
Brasier, C. M., Robredo, F. & Ferraz, J. F. P. (1993). *Plant Pathol.* **42**, 140–145.
Brünger, A. T., Adams, P. D., Clore, G. M., Delano, W. L., Gros, P., Grosse-Kunstleve, R. W., Jiang, J. S., Kuszewski, J., Nilges, M., Pannu, N. S., Read, R. J., Rice, L. M., Simonson, T. & Warren, G. L. (1998). *Acta Cryst.* D**54**, 905–921.
Duclos, J., Fauconnier, A., Coelho, A. C., Bollen, A., Cravador, A. & Godfroid, E. (1998). *DNA Seq.* **9**, 231–237.
Duclos, J., Trincão Aurélio, M., Graça, J., Coelho, A. C., Fauconnier, A., Jacquet, A., Bollen, A., Cravador, A., Biemans, R. & Godfroid, E. (1998). *Proceedings of the Twelfth Forum for Applied Biotechnology*, pp. 1695–1698. University of Gent, Belgium.
Eisenhaber, F., Lijnzaad, P., Argos, P., Sander, C. & Scharf, M. (1995). *J. Comput. Chem.* **16**, 273–284.
Evans, H. C. & Prior, C. (1987). *Outlook Agric.* **16**, 35–41.
Fefeu, S., Bouaziz, S., Huet, J. C., Pernollet, J. C. & Guittet, E. (1997). *Protein Sci.*, **6**, 2279–2284.
Gooley, P. R., Keniry, M. A., Dimitrov, R. A., Marsh, D. E., Keizer, D. W., Gayler, K. R. & Grant, B. R. (1998). *J. Biomol. NMR*, **12**, 523–534.

Grant, B. R., Ebert, D. & Gayler, K. R. (1996). *Australas. Plant Pathol.* **25**, 148–157.
Gregory, P. H. (1983). In *Phytophthora*, edited by D. C. Erwin, S. Bartnicki-Garcia & P. H. Tsao. St Paul, USA: American Phytopathological Society.
Holm, L. & Sander, C. (1993). *J. Mol. Biol.* **233**, 123–138.
Huet, J. C., Le Caer, J. P., Nespoulous, C. & Pernollet, J. C. (1995). *Mol. Plant-Microbe Interact.* **8**, 302–310.
Huet, J. C., Nespoulous, C. & Pernollet, J. C. (1992). *Phytochemistry*, **31**, 1471–1476.
Huet, J. C. & Pernollet, J. C. (1989). *FEBS Lett.* **257**, 302–306.
Huet, J. C., Sallé-Tourne, M. & Pernollet, J. C. (1994). *Mol. Plant-Microbe Interact.* **7**, 302–304.
Kamoun, S., Young, M., Glascock, C. B. & Tyler, B. M. (1993). *Mol. Plant-Microbe Interact.* **6**, 15–25.
Keller, H., Pamboukdjian, N., Ponchet, M., Poupet, A., Delon, R., Verrier, J. L., Roby, D. & Ricci, P. (1999). *Plant Cell*, **11**, 223–235.
Kraulis, P. (1991). *J. Appl. Cryst.* **24**, 946–950.
Kumar, S. & Rzhetsky, A. (1996). *J. Mol. Evol.* **42**, 183–193.
Large, E. C. (1940). *The Advance of the Fungi.* London: Cape.
Laskowski, R. A., MacArthur, M. W., Moss, D. S. & Thornton, J. M. (1993). *J. Appl. Cryst.* **26**, 283–291.
McBlain, B. A., Hacker, J. K., Zimmerly, M. M. & Schmitthenner, A. F. (1991). *Crop Sci.* **31**, 1412–1417.
McBlain, B. A., Zimmerly, M. M., Schmitthenner, A. F. & Hacker, J. K. (1991). *Crop Sci.* **31**, 1405–1411.
Marti-Renom, M. A., Stuart, A. C., Fiser, A., Sanchez, R., Melo, F. & Sali, A. (2000). *Annu. Rev. Biophys. Biomol. Struct.* **29**, 291–235.
Merritt, E. A. & Bacon, D. J. (1997). *Methods Enzymol.* **277**, 505–524.
Mikes, V., Milat, M. L., Ponchet, M., Panabières, F., Ricci, P. & Blein, J. P. (1998). *Biochem. Biophys. Res. Commun.* **245**, 133–139.
Mikes, V., Milat, M. L., Ponchet, M., Ricci, P. & Blein, J. P. (1997). *FEBS Lett.* **416**, 190–192.
Navaza, J. (1994). *Acta Cryst.* A**50**, 157–163.
Nespoulous, C., Huet, J. C. & Pernollet, J. C. (1992). *Planta*, **186**, 551–557.
Nicholls, A., Bharadwaj, R. & Honig, B. (1993). *Biophys. J.* **64**, A166.
Osman, H., Mikes, V., Milat, M. L., Ponchet, M., Marion, D., Prange, T., Maume, B. F., Vauthrin, S. & Blein, J. P. (2001). *FEBS Lett.* **489**, 55–58.
Osman, H., Vauthrin, S., Mikes, V., Milat, M. L., Panabières, F., Marais, A., Brunie, S., Maume, B., Ponchet, M. & Blein, J. P. (2001). *Mol. Biol. Cell*, **12**, 2825–2834.
Otwinowski, Z. & Minor, W. (1997). *The HKL Manual.* New Haven, CT, USA: Yale University Press.
Panabières, F., Ponchet, M., Allasia, V., Cardin, L. & Ricci, P. (1997). *Mycol. Res.* **101**, 1450–1468.
Perez, V., Huet, J. C., Nespoulous, C. & Pernollet, J. C. (1997). *Mol. Plant-Microbe Interact.* **10**, 750–760.
Perez, V., Huet, J. C., O'Donohue, M., Nespoulous, C. & Pernollet, J. C. (1999). *Phytochemistry*, **50**, 961–966.
Pernollet, J. C., Sallantin, M., Sallé-Tourne, M. & Huet, J. C. (1993). *Physiol. Mol. Plant Pathol.* **42**, 53–67.
Perrakis, A., Morris, R. & Lamzin, V. S. (1999). *Nature Struct. Biol.* **6**, 458–463.
Picard, K., Ponchet, M., Blein, J. P., Rey, P., Tirilly, Y. & Benhamou, N. (2000). *Plant Physiol.* **124**, 379–395.
Podger, F. D. (1972). *Phytopathology*, **62**, 972–981.
Podger, F. D., Doepel, R. F. & Zentmeyer, G. A. (1965). *Plant Dis. Rep.* **49**, 943–947.
Ponchet, M., Panabières, F., Milat, M.-L., Mikes, V., Montillet, J. L., Suty, L., Triantaphylides, C., Tirilly, Y. & Blein, J. (1999). *Cell. Mol. Life Sci.* **56**, 1020–1047.
Ramachandran, G. N. & Sasisekharan, V. (1968). *Adv. Protein Chem.* **23**, 283–438.
Ricci, P., Bonnet, P., Huet, J. C., Sallantin, M., Beauvais-Cante, F., Bruneteau, M., Billard, V., Michel, G. & Pernollet, J. C. (1989). *Eur. J. Biochem.* **183**, 555–563.
Roussel, A. & Cambillau, C. (1989). *TURBO-FRODO.* Silicon graphics Geometry Partners Directory, pp. 77–78.
Sali, A. & Blundell, T. L. (1993). *J. Mol. Biol.* **234**, 779–815.
Sánchez, M. E., Caetano, P., Ferraz, J. F. P. & Trapero, A. (2002). In the press.
Shea, S. R., Shearer, B. L., Tippet, J. T. & Deegan, P. M. (1983). *Plant. Dis.* **67**, 970–973.
Thompson, J. D., Higgins, D. G. & Gibson, T. J. (1994). *Nucleic Acids Res.* **22**, 4673–4680.
Vauthrin, S., Mikes, V., Milat, M. L., Ponchet, M., Maume, B., Osman, H. & Blein, J. P. (1999). *Biochim. Biophys. Acta*, **1419**, 335–342.
Wendehenne, D., Binet, M. N., Blein, J. P., Ricci, P. & Pugin, A. (1995). *FEBS Lett.* **374**, 203–207.
Yu, L. M. (1995). *Proc. Natl Acad. Sci. USA*, **92**, 4088–4094.